

LARBI HAMMADI1 AND ALAIN PONTON2*

'Laboratoire de Rhéologie, Transport et Traitement des Fluides Complexes (LRTTFC), Faculté d'Architecture et de Génie civil, Département d'Hydraulique, Université des Sciences et de la Technologie d'Oran (USTO) B.P. 1505 Oran-EL-M'naour 31000, Algérie

²Laboratoire Matière et Systèmes Complexes (MSC), Université Paris Diderot-Paris 7 & CNRS, Bâtiment Condorcet CC 7056, 75205 Paris Cedex 13, France

* Corresponding author: alain.ponton@univ-paris-diderot.fr

Received: 23.8.2016, Final version: 12.12.2016

ABSTRACT:

In this paper we investigate the rheological complex behavior of a vase of Fergoug dam which is located in the region Perregaux (Western Algeria) as a function of aging time, shear rate, and temperature. The modified Herschel-Bulkley model is used to fit the stationary flow curves of vase as a function of aging time and the generalized model of Kelvin-Voigt is successfully applied to fit the creep and recovery data and to analyze the viscoelastic properties of vase as a function of temperature. Finally the thixotropic behavior studied at constant temperature is analyzed by using the Herschel-Bulkley model including a structural parameter in order to account for time dependent effect. It is demonstrated that the increase in shear rate induces a restructuring and reorganization of the particles of the vase at the microstructural level.

KEY WORDS:

Vase of dam, soft matter, structural parameter, thixotropy, viscoelasticity

1 INTRODUCTION

The siltation of dams is a complex problem affecting all countries of all over the world in general, and Maghreb countries in particular with varying in the rate of silting that differ from one area to another. Algeria is a country well known by lack of water resources where the vase deposits in reservoirs of dams are estimated to 20 million m³ per year on average [1]. Therefore, their water storage capacity estimated at 6.2 billion m³ is reduced by 0.3% per year [2]. Mastering the techniques of dredging recovery of eroded vase requires an understanding of the rheological behavior of vase and the relationships with their physico-chemical characteristics. The vases of dams belong to the families of the sludge but with low organic content matter. In addition, the origin of the vases is directly related to the phenomena of soil erosion while the origin of sludge is directly related to water treatment in the sewage treatment plant. There is significant research activity in rheological of sewage sludge. Recently Baudez et al. [3] demonstrates that the rheological behavior of pasty sewage sludge at high concentration can be best fitted by a modified Herschel-Bulkley model. According to Hammadi et al. [4] and Baudez [5], the sludge suspension is also known to be strongly thixotropic material in which an apparent viscosity of the sludge depends on the shear rate and aging time. The viscoelastic properties of the digested sludge within the linear viscoelastic region were studied by Liu et al. [6] using frequency sweep tests. The digested sludge from reactors that received the pretreatment presented weaker solid-like properties (elastic characteristics) and the different reactor configurations have an impact on viscoelastic properties of sludge within the linear viscoelastic region. Baudez [7] studied effect of several parameters such as the time of rest, the slope of the shear rate ramp or the data sampling on thixotropic behavior of sewage sludge. It has been showed that higher ramping slopes and shorter data sampling times induce an increase of initial peak and the hysteresis area.

The impact of pH, temperature, solid concentration, and polymer dose on the rheology and flow behavior of thickened excess activated sludge has been studied by Hong et al. [8]. It has been clearly demonstrated that the decrease in concentration from 3.7 to 3.1%w/w resulted in a drastic reduction of yield stress from 27.6 to 11.0 Pa.

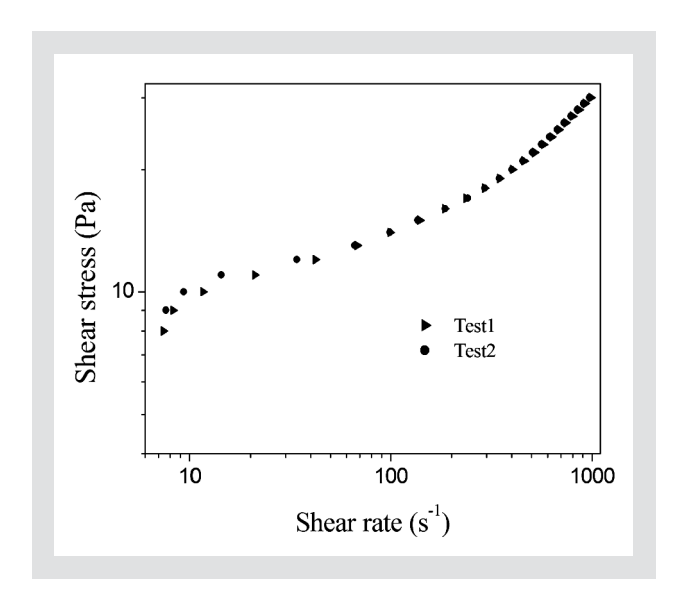


Figure 1: Repeatability of the measurements.

The increase of temperature from 25 to 55 °C caused a decrease of the Bingham plastic model parameters (yield stress and plastic viscosity) while the yield stress increased by increasing the pH of sludge. From the literature different rheological properties of the sludge have been investigated and analyzed by various models [9-11]. However, as far as we know results only obtained from empirical tests derived from methods used in soil mechanics have been published concerning vases of dams, in order to promote these vases in the field of construction. Only a few studies focused on the rheological behavior of vases. However knowledge of the rheological characteristics of the vases plays a fundamental role on flows and performance of transport technologies such as losses of linear and singular energy, non flow zones, recirculation time, and operation of desalting dams [12]. The vases of dam are similar to sludge and are non-Newtonian fluids with yield stress and rheological parameters such as viscosity depending on vase surface or temperature of vase, pH or ionic environment [13, 14]. In this paper, the rheological characteristics of vases of dam are studied as a function of aging time, shear rate and temperature with the objective of being used in industrial application. Thus, it can provide useful information for the proper design of pipes and the selection of pumps during hydraulic dredging operation of the dam, seeped of pumps and the period of dredging of dams.

2 MATERIALS AND METHODS

2.1.1 Recovered sample

The vase used in this study was recovered from the discharge area of Fergoug dam, located in the region Perregaux (Western Algeria) as a powder. It is the first dam which has been dredging in Algeria from 1986 to 1989 with more than 10 million m³ of dredged vase. The dredging was carried out as function of dredge floating. Vase is drawn by drag and expelled through a pipeline consisting of a floating part and affixed part on hun-

Chemicals	wt%
SiO ₂	53.30
Al_2O_3	6.29
Fe ₂ O ₃	1.76
MgO	0.21
CaO	16.64
SO ₃	0.11
Na₂O	0.69
K ₂ O	2.89
Loss of ignition	17.91

Table 1: Chemical analysis of vase samples in wt%.

dreds of meters in length. The chemical analysis of vase was carried out by the Public Works Laboratory of Oran (LTPO). The results are presented in Table 1.

2.1.2 Sample preparation

The vase as a powder was brought to the oven for 24 hours at 40 °C for dehydration then crushed and passes away a sieve of 80 μ m to perform a size sorting compatible with cone and plate geometry used for rheological measurements. A same experimental procedure was used for the preparation of all suspensions. First, vases powder was dispersed in the required amount of distilled water by continuous magnetic stirring at room temperature during 24 hours, as preliminary tests showed that this duration corresponded to the stabilization of the yield stress. One mass concentration of vase suspension (45 %) was studied.

2.2 EXPERIMENTAL SET UP

The rheological measurements were performed by using a torque controlled rheometer (MARS II from Thermo-Fisher) connected to a temperature controlled water bath and equipped with a cone-plate geometry (diameter: 35 mm, angle: 2 degree, and gap: $104 \mu m$). A solvent trap was placed around the measuring device in order to minimize solvent evaporation (water).

2.3 EXPERIMENTAL PROCEDURES

2.3.1 Effect of aging time

The evolution of the rheological properties of the vase with the different aging times was investigated to obtain some information about the stability. In order to avoid any memory effect, the sample was pre-sheared at a constant shear rate of 30 s⁻¹ during 60 s. After this pre-shearing, the sample was kept at rest during 600 s prior to measurements in order to allow the material to recover, at least partially, its initial structure. The imposed shear stress range depends on the mass concentration of vase [4]. Consequently, the flow experimental procedure consists of a linear ramp of increasing stresses from 1 to 30 Pa over 50 minutes at constant temperature (20 ± 0.2 °C). In order to test the reproducibility of results, two replicates were performed for most of the experiments. An example is shown in Figure 1. In all cases, the maximum difference between two replicates is 2 %.

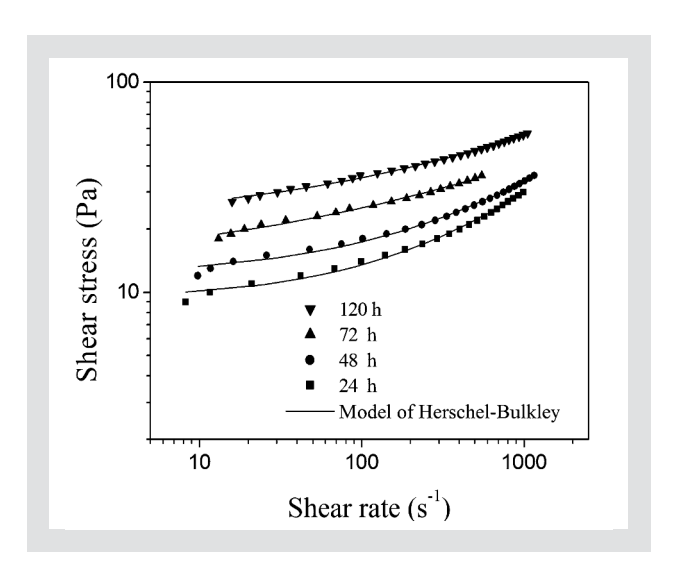


Figure 2: Shear stress as a function of shear rate at 20 $^{\circ}$ C for different aging times. The solid lines correspond to the curve fitting to Equation 1.

2.3.2 Apparent viscosity evolution under constant shear rate

After a rest time (time during which the sample is left at rest under geometry) of 600 s, the samples were sheared during 300 s at different constant shear rates (15, 20, 25, and 30 s⁻¹) at constant temperature (20 \pm 0.2 °C). A new fresh sample was used for each applied shear rate in order to avoid any irreversible evolution of the vases.

2.3.3 Creep and recovery tests

After a rest time of 600 s, creep and recovery tests were performed by first applying a constant shear stress at different values between 2 and 9.5 Pa during 300 s to the samples of vase and then removing the shear stress during 300 s in order to obtain the time dependence of the compliance *J*.

3 RESULTS AND DISCUSSION

3.1 EFFECT OF AGING TIME

The variation of the shear stress τ as a function of the shear rate $\dot{\gamma}$ at different aging times (time during which the sample is left in the laboratory at ambient conditions) from 24 to 120 hours for the studied sample of vase clearly shows two behaviors separated by a critical shear rate: a Non-Newtonian behavior after a yield stress followed by a plastic behavior (Figure 2). It should be noted that preliminary tests were performed by measuring the flow properties every one hour after preparation of samples. We obtained a good repeatability of measurements only after a rest time of 24 hours. Experimental data were fitted to modified Herschel-Bulkley model developed by Baudez et al. [3], which has been successfully employed for anaerobic digested sludge (Figure 2):

$$\tau = \tau_o + K \dot{\gamma}^n + \eta_B \dot{\gamma} \tag{1}$$

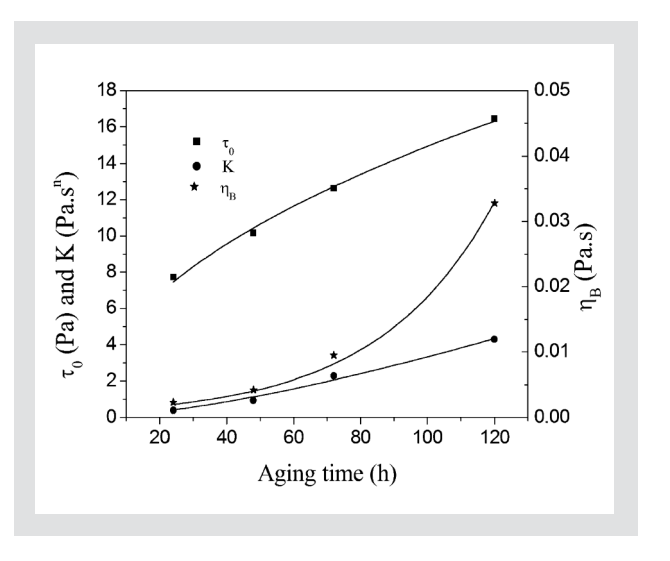


Figure 3: Yield stress τ_o , consistency index K and Bingham viscosity η_B as a function of aging time of vase. The solid lines correspond to the curve fittings to Equations 2 to 4.

where τ_o is the yield stress in Pa, K the consistency index in Pasⁿ, n the flow index, and η_B the Bingham viscosity in Pas.

3.1.1 Effect of aging time on the rheological parameters of vase

In the studied range of aging times, the increase of yield stress and the consistency index of vases are well described by a power law while Bingham viscosity increases with aging time following an exponential law (Figure 3):

$$\tau_{o} = \tau_{toag} t_{ag}^{\alpha_{1}} \tag{2}$$

$$K = K_{toag} t_{ag}^{\alpha_2} \tag{3}$$

$$\eta_{B} = \eta_{B_{t \circ ag}} \exp\left(\alpha_{3} t_{ag}\right) \tag{4}$$

where τ_{toag} = 1.58 Pa, K_{toag} = 0.004 Pasⁿ, and $\eta_{B_{toag}}$ = 0.001 Pas are respectively the yield stress, consistency index, and Bingham viscosity at aging time equal zero. α_1 = 0.49 h^{-1} , α_2 = 1.46 h^{-1} , and α_3 = 0.03 h^{-1} s are power law index which are independent on the shear rate. Concerning the flow index (Equation 1), it is found constant and equal to 0.39. Similar behavior have already been observed as a function of concentrations of sludges and mud suspensions [3, 5, 15, 16].

3.1.2 Effect of aging time on the apparent viscosity of vase The apparent viscosity is calculated for different shear rates and different aging times of vase. For all tested shear rates we observed an increase of apparent viscosity as a function of aging time which is well described by a power law:

$$\eta = \eta_{t \circ ag} t_{ag}^{\alpha_{\circ}} \tag{5}$$

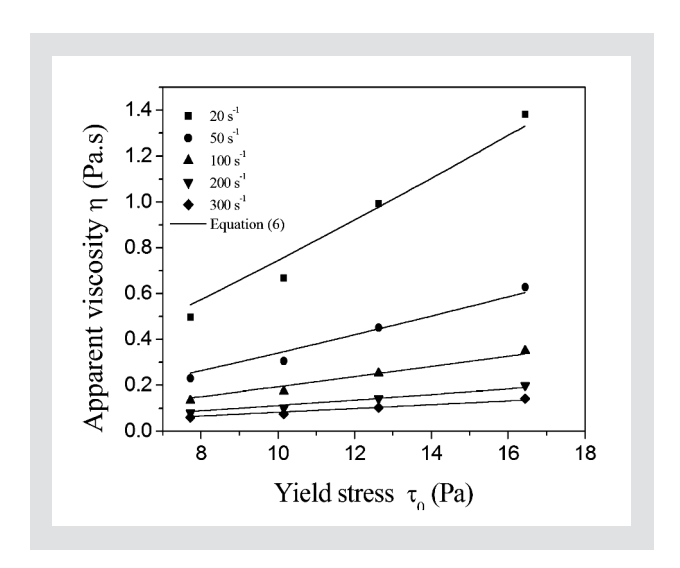


Figure 4: Variation of apparent viscosity η as a function of yield stress τ_o . The solid lines correspond to curve fitting to Equation 6.

where η_{toag} of the apparent viscosity in Pas at aging time equal zero t_{oag} = 0 and α_o is a power law index which depends on the shear rate in h^{-1} . Equation 5 can also be written in terms of initial viscosity and yield stress as follows:

$$\eta = \eta_{toag} \left(\frac{\tau_o}{\tau_{toag}} \right)^{\frac{\alpha_o}{\alpha_1}}$$
 (6)

As shown in Figure 4, the apparent viscosity increases with increasing the yield stress. If a vase is left a long period of time in the dam, the yield stress τ_o and the apparent viscosity tend to the infinite that can cause problems during dredging operation of dam (pump blocking).

3.1.3 Master curve

Considering the self-similar shapes of the flow curves (Figure 2), experimental data are plotted by using a tangential stress dimensionless $T = \tau/\tau_o$ and a dimensionless shear rate $\Gamma = \eta_B \dot{\gamma} / \mu \tau_o$ with μ is the viscosity of equivalent suspension of force-free particles in water [17, 18] and assume its value as the value 1 Pas. As shown in Figure 5 a master curve is observed in the dimensionless diagram (Γ , T) for different aging times. For low values of Γ (Γ < 24) the flow curve corresponds to a threshold behavior which may be represented by the following dimensionless equation:

$$T = 1 + \phi \, \Gamma^m \tag{7}$$

where ϕ and m are parameters of the material which depends on the time characteristics of the rupture and reformation of links but not depending on the aging time of vase, for this study ϕ =0.23 and m =0.51. For high values of Γ (Γ > 24) the flow curve corresponds to a Newtonian behavior. By analogy with the effect of concen-

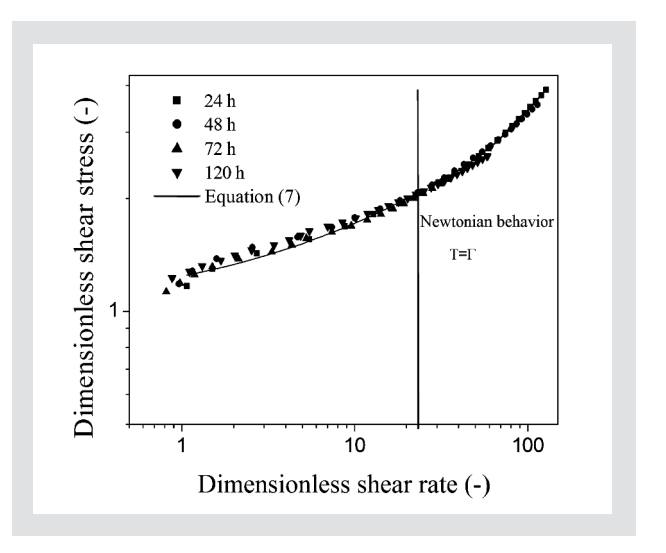


Figure 5: Dimensionless flow curves in the dimensionless diagram (Γ, T) for different aging times.

tration cited in literature, it could be concluded that increasing the aging time does not change the nature of the two kinds of interactions within the vase [19]: Hydrodynamic interactions between solid particles and surrounding fluid (Bingham viscosity) and non-hydrodynamic interactions between solid particles (yield stress). Moreover the master curve allows to predict the variation of shear stress as a function of shear rate at a given aging time with the only knowledge of the initial yield stress at aging time equal zero.

3.2 APPARENT VISCOSITY EVOLUTION UNDER CONSTANT SHEAR RATE AND DETERMINATION OF THE STRUCTURAL PARAMETER

Figure 6 shows the variation of apparent viscosity for vase of dam as a function of time of shearing at different constant shear rates and at constant aging time of 24 hours. For all studied shear rates, the viscosity decreases significantly with time of shearing, particularly in the initial stages of shear. After a shearing period of 150 s, the viscosity tends to an equilibrium value. This behavior could be due to the flocculation or deflocculation of the of vase particle with shearing in water [20].

In order to analyze the structural evolution of the vase, we applied the phenomenological model of Tiu and Boger [21] based on an approach initially suggested by Moore [22] and refined by Cheng and Evans [23]. This choice was motivated by the simplicity (minimum number of parameters) and efficiency of this model. Cheng and Evans argued that the stress-strain equation depends on the fluid model and must be completed with a kinetic equation of structural parameter λ changing with time of shearing. This parameter describes the current state of agglomeration. As pointed out before, the flow curves of vase were found to be well fitted by the modified model of Herschel-Bulkley with good agreement (see Figure 2). Following the model proposed by Tiu and Boger [21], the Herschel-Bulkley

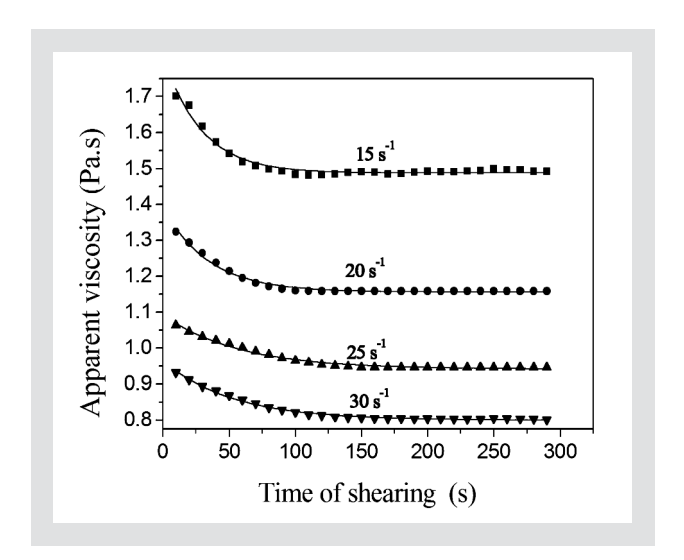


Figure 6: Viscosity of vase as a function of time of shearing at 20 °C for constant shear. The solid line corresponds to curve fitting to Equation 18.

model was modified to take into account of state of vase and it is assumed to be:

$$\tau(t) = \lambda(t)\tau_{zero} \tag{8}$$

The shear stress at zero time of shear τ_{zero} was given by a Herschel Bulkley model:

$$\tau_{zero} = \tau_{yo} + K_{,\dot{\gamma}^n} \tag{9}$$

Combining Equations 8 and 9 yields:

$$\tau(t) = \lambda \left(\tau_{yo} + K_{,i} \dot{\gamma}^{n} \right) \tag{10}$$

For their rate equation Tiu and Boger [21] used a second-order kinetic equation:

$$\frac{d\lambda}{dt} = -k_2 \left(\lambda - \lambda_e\right)^2 \quad \text{for} \quad \lambda > \lambda_e \tag{11}$$

The structural parameter λ ranged from an initial value of unity for zero shear time to an equilibrium value λ_e lower than unity. The rate constant k_2 is a function of shear rate that should be determined experimentally

γ (s ⁻¹)	a ₁ (Pa ⁻¹ s ⁻²)	K ₂ (s ⁻¹)*	η _o (Pas)	η _e (Pas)	$\lambda_{\rm e} = \eta_{\rm e}/\eta_{\rm o}$
15	0.088	0.153	1.821	1.488	0.817
20	0.109	0.145	1.394	1.156	0.828
25	0.126	0.136	1.125	0.941	0.836
30	0.139	0.129	0.947	0.8	0.844

Table 2: Variation of a_1 , K_2 , η_0 , η_e , and λ_e as a function of shear rate (* experimentally).

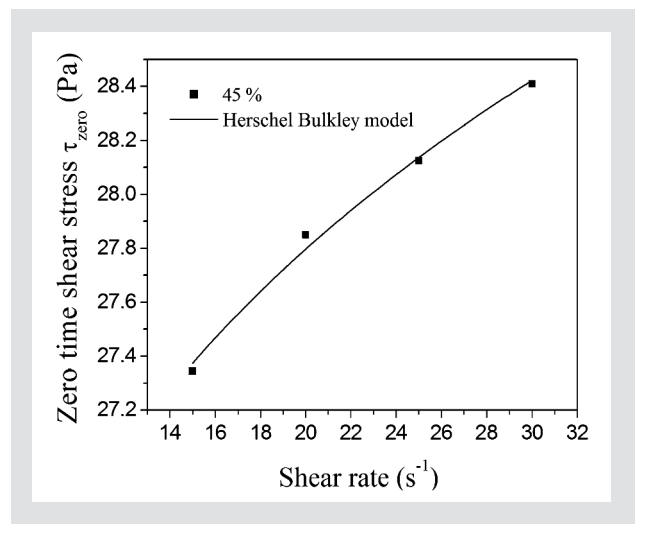


Figure 7: Zero time shear stress τ_{zero} of vase as a function of shear rate. The solid line corresponds to curve fitting to Equation 12.

(see Table 2). Then entire time-dependent behavior of the vase might be completely described by Equations 10 and 11 with the parameters τ_{yo} , K_1 , n_1 , and k_2 evaluated from experimental data. The rheological constants τ_{yo} , K_1 , and n_1 are determined with initial shearing conditions ($\lambda=1$ and t=0) and Equation 10 reduces to the classical Herschel-Bulkley equation [24]. In other words, they are determined from the initial shear stress in the material at the beginning of a rheological test for each studied shear rate. Figure 7 shows the zero shear stress τ_{zero} at a function of shear rate. The curve was fitted to the model of Herschel-Bulkley. The resulting equation is:

$$\tau_{zero} = 21.98 + 2.7 \dot{\gamma}^{0.25}$$
 with $R^2 = 0.991$ (12)

To determine the rate constant k_2 experimentally, Equation 11 can be integrated analytically under conditions of constant shear rate to yield:

$$\frac{1}{\lambda - \lambda_e} = \frac{1}{\lambda_o - \lambda_e} + K_2 t \tag{13}$$

The instantaneous apparent viscosity for any fluid is defined by:

$$\eta = \frac{\tau}{\dot{\gamma}} \tag{14}$$

Combining Equations 10 and 14 yields:

$$\lambda = \frac{\eta \dot{\gamma}}{\tau_{yo} + K_{,i} \dot{\gamma}^{n_{i}}} \tag{15}$$

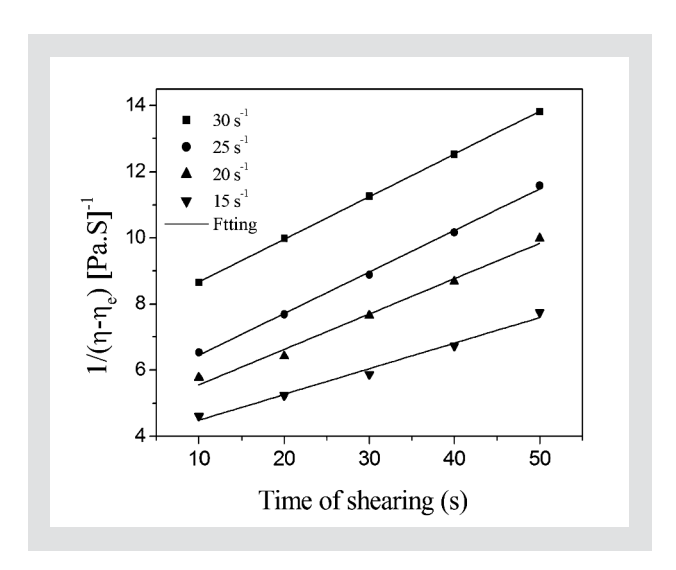


Figure 8: Linear relationship between $1/(\eta-\eta_e)$ and time for different shear rates .The solid line corresponds to a fitting of data by linear regression.

Equation 15 is also valid at initial and equilibrium conditions in which λ and η are replaced by λ_o and η_o and by λ_e and η_e , respectively. Substituting Equation 15 into Equation 13 yields:

$$\frac{1}{\eta - \eta_e} = \frac{1}{\eta_o - \eta_e} + a_1 t \tag{16}$$

where

$$a_{1} = \frac{k_{2}\dot{\gamma}}{\tau_{yo} + K_{1}\dot{\gamma}^{n_{1}}}$$
 (17)

The equilibrium viscosity η_e was obtained by fitting the time dependence of the viscosity (Figure 6) by an exponential decay curve [25] of the form:

$$\eta = \eta_e + (\eta_o - \eta_e) exp(-\beta t)$$
(18)

where β is the rate constant in (s-1). Therefore, for a given shear rate, a plot of $1/(\eta-\eta_e)$ versus time of shearing t (Figure 8) should yield a straight line with a slope equal to a_1 . Repeating the same procedure at other shear rates will establish the relationship between a_1 and $\dot{\gamma}$ and hence K_2 , and $\dot{\gamma}$ from Equation 18. Table 2 shows the variation of a_1 , K_2 , η_o , η_e , and λ_e with shear rate. The structural parameter λ is deduced from Equation 16 and writes:

$$\lambda = \lambda_e + \frac{1}{\frac{1}{(1 - \lambda_e)} + K_2 t}$$
(19)

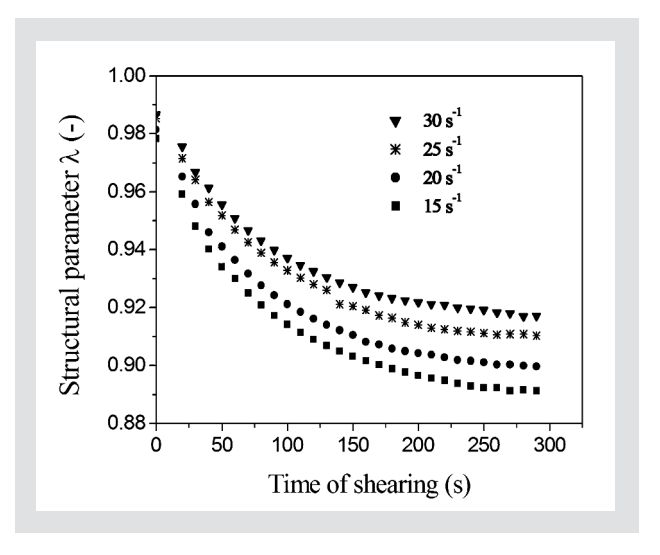


Figure 9: Structural parameter as a function of time of shearing at 20 °C for different shear rates.

As shown in Figure 9 structural parameter changes are most significant during the initial shear period after which nearly constant values are reached. We also find that structural parameter of vase suspension increases with increasing the shear rate. This behavior could be explained by the deflocculation of particles of vase in the water at high shear rate leading to an enhance organization of the particles of the vase at the microstructural level as suggested by Chen et al. [26].

3.3 EFFECT OF TEMPERATURE ON CREEP AND RECOVERY OF VASE

Figure 10 shows the values of compliance $J(t) = \gamma/\tau$ as a function of time, for the creep experiments corresponding to the vase studied for temperature range between 5 and 30 °C, in a time interval between o and 300 s. For the interval time between 300 and 600 s, we have represented the corresponding recovery. The observed decrease of the elastic compliance (increase of the elastic modulus G = 1/J) with the increase of temperature is related to an increase of the viscoelastic properties of vase. In other words, the creep deformation decreases with increasing the temperature and the time necessary to reach a constant deformation during recovery after removal of the shear stress decreases. The elastic properties were defined by correlating the results with the well-known viscoelastic models of Burger model or Generalized Kelvin-Voigt model [25, 27], based on the association in series of the Maxwell model and the Kelvin-Voigt. The creep curves are described by:

$$J_{F} = J_{o} + \frac{t}{\mu_{o}} + \sum_{i=1}^{N} J_{i} \left[1 - exp\left(-\frac{t}{\theta_{i}} \right) \right]$$
(20)

$$\theta_i = \frac{J_i}{\eta_i} \tag{21}$$

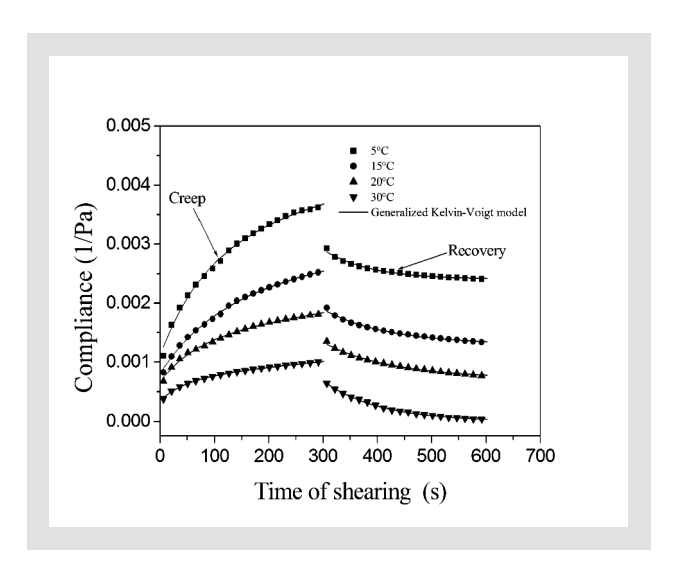


Figure 10: Compliance versus time in creep and recovery test at different temperatures of vase. The solid lines correspond to the curve fitting to generalized Kelvin-Voigt model Equations 20 and 22 with N=1.

Whereas the recovery strain is given by:

$$J_{R} = \frac{t_{1}}{\mu_{o}} + \sum_{i=1}^{N} J_{i} \left[exp\left(\frac{t_{1}}{\theta_{1}}\right) - 1 \right] exp\left(-\frac{t}{\theta_{i}}\right)$$
(22)

where J_o is the purely elastic contribution (or the instantaneous elastic compliance), μ_o is the purely viscous contribution, represented by the dashpot of the Maxwell model, i.e. the uncoupled or residual steady-state viscosity obtained from the creep curve at long times when the compliance curve is linear, J_i is the contribution to delayed elastic compliance, θ_i is the retarded time, η_i is the delayed viscosity and t_1 is the time where the stress is applied for $t \le t_1$ and removed at $t = t_1$. The fittings of experimental data in Figure 10 were performed with just one Kelvin-Voigt solid (N = 1) and the fitting parameters are detailed in Table 3. The column $G_1 = 1/J_1$ represents the instantaneous elastic modulus of the Maxwell unit at t = 0 or the instantaneous elastic response of the system and the column $G_o = 1/J_o$ is the elastic modulus of Kelvin-Voigt. The latter represents the contributions of the retarded elastic region to the total compliance. The observed strong increase of G_o and G_1 when the temperature is increased between 5 and 30 °C is related to a transition from viscous to elastic behavior and an increase of the viscoelastic properties in the studied range of temperature. This behavior could be explained by the

emp. (°C)	G _o (Pa)	G ₁ (Pa)	μ _o (Pas)	G ₁ (Pa)	μ_{O} (Pas)	θ_1 (s)
	901	513	436951	1923	124673	85
5				-		116
						127 208
	500	1235 0 1493	1235 730 1493 1351	1235 730 668321 1493 1351 685973	1235 730 668321 1562 1493 1351 685973 1471	5 1235 730 668321 1562 230004 0 1493 1351 685973 1471 415497

Table 3: Fitting parameters of the creep-recovery data in Figure 10, with N = 1 in Equations 20 and 22.

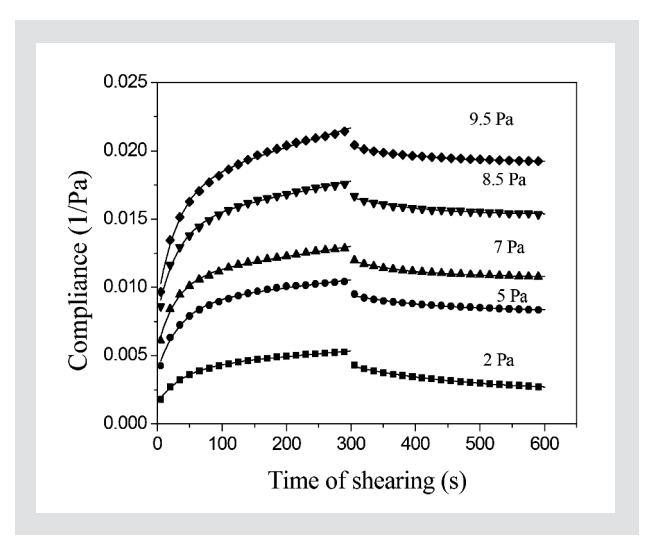


Figure 11: Compliance versus time of shearing in creep and recovery tests at different applied stresses on vase (45 %). The solid lines correspond to the curve fitting to generalized Kelvin-Voigt model Equations 20 and 22 with N=1.

interaction between the particles of the vase suspension [28, 29]. Concerning μ_o let us mention that it has the meaning of viscosity of the system in the Newtonian regime, whereas it also shows a clearly increasing trend as the temperature of vase is increased. This increasing of viscosity could be explained by the interactions between particles of vase and the enhancement of Brownian motion [30]. At high temperature, the applied stress of 2 Pa is not sufficient to break particle-to-particle bonds, and the suspensions do not flow with a high viscosity. At low temperature such resistance to flow is not so large, and this explains the lower values of μ_o and G_τ . The characteristic relaxation time θ_τ associated with these breaking/reconstruction processes does not show a definite trend when estimated from creep data.

3.4 EFFECT OF APPLIED STRESS ON CREEP AND RECOVERY OF VASE

After a rest time (time during which the sample is left at rest in geometry) of 600 s, in the creep phase, samples were subjected to different constant stresses (2, 5, 7, 8.5, and 9.5 Pa) and at constant temperature (20 °C). In the recovery phase, the applied stress was suddenly removed and sample recovery was measured for an additional period of 300 s. As can be observed in Figure 11, the increasing of stress from 2 to 9.5 Pa caused an increase on the elastic compliance of vase. The Generalized Kelvin-Voigt model (Equations 20 and 22) has been

Stress (Pa)	Creep G _o (Pa)	G ₁ (Pa)	μ _o (Pas)	Recovery G ₁ (Pa)	μ _o (Pas)	θ_1 (s)
2	1493	1351	685973	1471	415497	127
5	956	804	176495	833	36403	120
7	781	696	132083	769	27932	104
8.5	625	449	100789	614	19571	98
9.5	411	219	71702	411	15634	93

Table 4: Fitting parameters of the creep-recovery data in Figure 11, with N = 1 in Equations 20 and 22.

applied to fit the experimental data and the fitting parameters are detailed in Table 4. A decrease of G_o and G_τ by a factor of 3.6 and 6 respectively is observed when the stress is increased from 2 to 9.5 Pa. In the same manner the viscosity (μ_o) is divide by 10. This transition from solid-like to fluid-like behaviors could be explained by a breaking of particle-to-particle bonds.

4 CONCLUSIONS

The stationary, thixotropic and viscoelastic behavior of vase was study as a function of aging time, shear rate and temperature. The stationary non-Newtonian flow behavior of vase was successfully modeled using the coupled Herschel-Bulkley and Bingham models over the studied range of aging times. The yield stress and the consistency index increased with the aging time according to a power law while the Bingham viscosity followed an exponential law with aging time. A master curve was obtained by using dimensionless shear stress and dimensionless shear rate. The rheological flow behavior of the vase can be then predicted at any aging time by the only knowledge of the initial yield stress at aging time equal zero. For practical dredging operation of dams, it could be then deduced to reduce dredging time of the dams as much as possible.

For low shear rates at a temperature of 20 °C a thixotropic behavior was observed. This behavior was analyzed by the simple model of Hershel-Bulkley modified by introducing a structural parameter λ which was found to increase with the applied shear rates. This increase of the structural parameter could be associated to a restructuring and reorganization of the particles of the vase. This later could induce a problem during the dredging operation of dams (blocking of pumps) and should be avoided by pumping the vases at high speeds in order to facilitate the flow of the vases.

A strong increase of elastic modulus deduced from creep measurements fitted to generalized Kelvin Voigt model with one element was observed when the temperature is increased between 5 and 30 °C. This behavior could be explained by an increase of the interactions between particles of vase due to an increase of the intensity of Brownian motion creating a problem during the dredging operation of dams. In order to facilitate the process of pumping the vases, we thus propose to drag this vase in winter period. The increase of shear stress induces a decrease of viscoelastic behavior of vase and breaking of particle-to-particle bonds. This later facilitates the process of pumping the vases. Consequently dragging this vase at pressure higher than the hydrostatic pressure of vase would make easier the process of pumping the vases.

REFERENCES

- [1] Khanchoul K, Boukhrissa Z, Acidi A, Altschul R: Estimation of suspended sediment transport in kebir drainage basin, Algeria, Quaternary International 262 (2012) 25 31.
- [2] Drouiche N, Ghaffour N, Naceur MW, Mahmoudi H, Ouslimane T: Reasons for the fast growing seawater desalination capacity in Algeria, Water Resources Management 25 (2011) 2743 – 2754.
- [3] Baudez C, Markis F, Eshtiaghi N, Slatter P: The rheological of anaerobic digested sludge, Water Res. 17 (2011) 5675–5680.
- [4] Hammadi L, Ponton A, Belhadri M: Temperature effect on shear flow and thixotropic behavior of residual sludge from wastewater treatment plant, Mech. Time-Depend. Mater. 17 (2013) 401–412.
- [5] Baudez JC: Physical aging and thixotropy in sludge rheology, Appl Rheol. 18 (2008) 13495.
- [6] Liu J, Yu D, Zhang J, Yang M, Wang Y, Wei Y, Tong J: Rheological properties of sewage sludge during enhanced anaerobic digestion with microwave-H₂O₂ pretreatment, Water Res. 98 (2016) 98–108.
- [7] Baudez JC: About peak and loop in sludge rheograms,J. Environ. Management 78 (2006) 232 239.
- [8] Hong E, Yeneneh AM, Kayaalp A, Sen TK, Ang HM, Kayaalp M: Rheological characteristics of municipal thickened excess activated sludge (TEAS): impacts of pH, temperature, solid concentration and polymer dose, Res. Chem. Intermed. 42 (2016) 6567–6585.
- [9] Wang YL, Dentel SK: The effect of high speed mixing and polymer dosing rates of the geometric and rheological characteristics of conditioned anaerobic digested sludge (ADS), Water Res. 44 (2010) 6041–6052.
- [10] Pevere A, Guibaud G, Goin E, Van Hullebusch E, Lens P: Effects of physico-chemical factors on the viscosity evolution of anaerobic granular sludge, Biochem. Eng. J. 42 (2009) 231–238.
- [11] Tixier N, Guibaud G, Baudu M: <u>Determination of some</u>
 rheological parameters for the characterization of activated sludge, Bioresource Technol. 90 (2003) 215–220.
- [12] Hammadi L, Ponton A, Belhadri M: Rheological study and valorization of waste sludge from wastewater treatment plants in the dredging operation of hydraulic dams, Energy Procedia 6 (2011) 302–309.
- [13] Lotito V, Lotito AM: Rheological measurements on different types of sewage sludge for pumping design, J. Environ. Management 137 (2014) 189–196.
- [14] Wang HF, Hu H, Yang HY, Zeng RJ: <u>Characterization of anaerobic granular sludge using a rheological approach</u>, Water Res. 106 (2016) 116–125.
- [15] Coussot P, Piau JM: On the behavior of fine mud suspensions, Rheo. Acta 33 (1994) 175 184.
- [16] Eshtiaghi N, Flora Markis F, Yap SD, Baudez JC, Slatter P: Rheological characterisation of municipal sludge: A review, Water Res. 47 (2013) 5493-5510.
- [17] Coussot P: Structural similarity and transition from Newtonian to non-Newtonian behavior for clay-water suspensions, Phys. Rev. Lett. 20 (1995) 3971–3974.
- [18] Baudez JC, Ayol A, Coussot P: Practical determination of the rheological behavior of pasty biosolids, J. Environ. Management 72 (2004) 181–188.

- [19] Baudez JC, Coussot P: Rheology of aging, concentrated, polymeric suspensions: Application to pasty sewage sludges, J. Rheol. 45 (2001) 1123–1139.
- [20] Markis F, Baudez JC, Parthasarathy R, Slatter P, Eshtiaghi N: The apparent viscosity and yield stress of mixtures of primary and secondary sludge: Impact of volume fraction of secondary sludge and total solids concentration, Chem. Eng. J. 288 (2016) 577–587.
- [21] Tiu C, Boger DV: Complete rheological characterisation of time dependent food products, J. Texture Stud. 3 (1974) 329 338.
- [22] Moore F: The rheology of ceramic and slip bodies, Trans. Brit. Ceram. Soc. 58 (1959) 470 494.
- [23] Cheng DCH, Evans F: Phenomenological characterization of the rheological behaviour of inelastic reversible thixotropic and antithixotropic fluids, Brit. J. Appl. Phys. 16 (1965) 1599 1617.
- [24] Butler F, McNulty P: Time dependent rheological characterisation of buttermilk at 5 °C, J. Food Eng. 25 (1995) 569 580.

- [25] Hammadi L, Boudjnanne N, Belhadri M: Effect of polyethylene Oxide (PEO) and shear rate on rheological properties of bentonite clay, Appl. Clay Sci. 99 (2014) 306 311.
- [26] Chen LB, Ackerson BJ, Zukoski CF: Rheological consequences of microstructural transitions in colloidal crystals, J. Rheol. 38 (1994) 193–216.
- [27] Dolz M, Corrias F, Díez-Sales O, Casanovas A, Hernández MJ: Influence of test times on creep and recovery behavior of xanthan gum hydrogels, Appl. Rheol. 19 (2009) 34201.
- [28] Coussot P, Ancey C: Rheophysical classification of concentrated suspensions and granular pastes, Phys. Rev. E 59 (1999) 4445–4457.
- [29] Song Z, Li T, Wang Q, Pan Y, Li L: Influence of microbial community structure of seed sludge on the properties of aerobic nitrifying granules, J. Environ. Sci. 35 (2015) 144–150.
- [30] Morariu M, Bercea M: Effect of temperature and aging time on the rheological behavior of aqueous poly(ethylene glycol)/Laponite RD dispersions, J. Phys. Chem. B 116 (2011) 48–54.

